EVS27
Barcelona, Spain, November 17-20, 2013

Friction Coefficients of Battery Metals and the Usage in Ultrasonic Welding Simulations

Wayne Cai[1], Peter J. Blau[2], Jun Qu[2]
[1]*General Motors R&D Center, 30500 Mound Rd, Warren, MI 48090, USA, wayne.cai@gm.com*
[2]*Oak Ridge National Laboratory, P.O. Box 2008, MS-6063, Oak Ridge, TN 37831, USA, blaupj@ornl.gov*
[2]*Oak Ridge National Laboratory, P.O. Box 2008, MS-6063, Oak Ridge, TN 37831, USA, qujn@ornl.gov*

Abstract

Ultrasonic welding is one of the mainstream joining technologies for an automotive battery pack where battery cells are welded mostly in series with bus-bars on interconnect circuit boards in battery electric vehicles (BEV). Mathematical simulations, such as Finite Element Analysis, have been used to simulate the ultrasonic welding for process and joint quality optimizations. Since friction-generated heat plays a critical role in ultrasonic welding, accurate friction coefficient measurement is essential to the fidelity of such simulations. This paper describes the experimental results of friction coefficients for such materials, as well as the effects of surface conditions, sliding frequencies, and normal loads on the friction coefficient. It was found that the average friction coefficient between a Cu bus-bar and a Cu tab is 1.2, while between a Cu bus-bar and an Al tab is 0.6. The finite element analysis of the battery tab welding process using the measured friction data is depicted.

Keywords: Friction, Copper, Aluminium, Battery Metal

1 Introduction

Ultrasonic metal welding produces a joint by applying clamping pressure and tangential vibration to the workpiece [1]. The process involves compression loading in the workpiece normal direction, cyclic loading in the tangential direction, and consequently heat generation and vibration due to friction between workpiece. Due to its advantages of welding dissimilar materials and multiple thin sheets, the technique has been used as one of the mainstream joining methods for an automotive battery pack where hundreds or even thousands of battery cells are welded in series with bus-bar coupons on interconnect circuit boards in order to meet the desired power and capacity for battery electric vehicles (BEV). Figure 1 ([2]) depicts GM's Chevrolet Volt battery tab welding configuration, with three aluminium battery tabs, three copper battery tabs, and a copper bus-bar in between. Prior research was conducted to understand and optimize the ultrasonic welding process from mechanical, thermal, and vibratory perspectives, e.g., [2, 3, 4, 5]. It is well-known that heat generation from friction is a major contributor to the weld quality. However, friction coefficients are not readily available for certain materials (i.e., Nickel coated copper for bus-bars and negative battery tabs, and anodized aluminium for positive battery tabs).

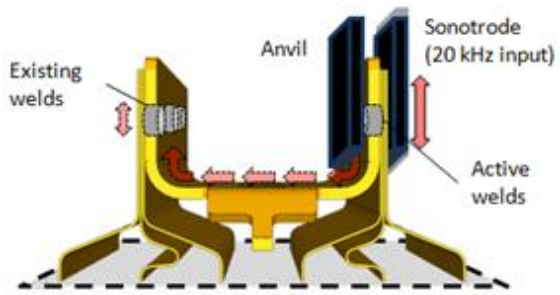

Figure 1 GM Chevrolet battery tab welding

A number of studies have investigated friction coefficient on the contact surface of different materials. Of the studies, Jairo et al. [6]

investigated kinetic friction coefficient on the interface of polycarbonate blade and flat rubber-belt when interacting with ore, lubricant, and pressure. Qu et al. [7] designed a pin-on-twin reciprocating wear test for heavy-duty diesel fuel injectors. Guermazi et al. [8] studied friction and wear behaviours on the static and kinetic contact of a steel ball against a polyethylene coating. Lee et al. [9] examined the friction and wear behaviour on the static and kinetic contact of a steel ball against a polycarbonate half-plane, as well as developed a finite element method to study friction and wear mechanisms. Siddiq and Ghassemieh [10] simulated ultrasonic welding of one sheet of aluminium on an aluminium substrate using Abaqus. Elangovan et al. [11] conducted numerical simulations on ultrasonic welding of two aluminium sheets to investigate effects of ultrasonic welding parameters on temperatures of the workpieces. Zhang and Li [12] conducted a dynamic temperature-displacement coupled analysis for ultrasonic welding of one sheet of aluminium on an aluminium substrate. Lee et al. [13] used a hybrid explicit/implicit finite element analyses to study the heat generation due to fiction in ultrasonic welding, as well as predict the weld quality for multiple, thin battery tabs joining.

This paper presents the experimental measurement results of friction coefficients for battery materials, as well as the effect of surface conditions, sliding frequencies, and normal loads on friction coefficients under laboratory test conditions that attempted to simulate the application. In our experiments, sliding (with a cyclic or reciprocating movement pattern) frequency was set at 2 Hz or 10 Hz; and normal load was set at 20 N, 60 N, or 100 N. 10Hz and 100N are the upper limits of sliding frequency and normal load that the friction tester can provide, though they are significantly lower than the vibration frequency (20 KHz) and welding force in a typical ultrasonic metal welding. Finally, a brief account of finite element analyses of ultrasonic welding for battery tabs follows.

2 EXPERIMENTAL DETAILS

2.1 Materials

As shown in Figure 2, the materials used in our experiments include:

- Cu bus-bar coupons ("Cu coupons"), with a thin layer of Nickel coating. Flat Cu coupons were used in this study to accommodate the friction test machine.
- Cu battery tabs ("Cu tabs"), with a thin layer of Nickel coating.
- Al battery tabs ("Al tabs"), with a thin layer of surface anodizing.

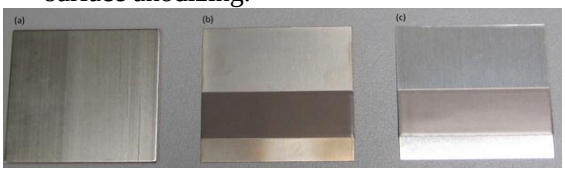

Figure 2 (a) Cu coupon; (b) Cu tab; (c) Al tab

We measured the surface roughness Cu coupons and battery tabs using a laser microscope scanner (Keyence VK-9710 with a Nikon 10X/0.30 WD 16.5 lens). The laser intensity photos are shown in Figure 3.

The surface roughness values are shown in Table 1, including highest peak (Rp), lowest valley (Rv), maximum height (Rz), arithmetic mean height (Ra), and root mean square height (Rq). For each material, the measurement was repeated five times for which the average and standard deviation are given in the table.

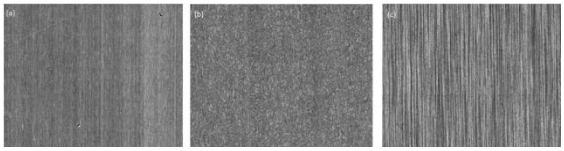

Figure 3 Laser intensity photos of (a) Cu coupon; (b) Cu tab; (c) Al tab

Table 1 Roughness measurement of Cu coupons and Cu/Al tabs (unit: microns)

	Materials	R_p	R_v	R_z	R_a	R_q
Average	Cu coupon	7.370	8.293	15.659	1.276	1.609
	Cu tab	6.097	6.021	12.118	1.046	1.312
	Al tab	9.715	8.777	18.493	1.236	1.557
Standard deviation	Cu coupon	1.138	1.766	2.607	0.114	0.153
	Cu tab	0.653	1.363	1.978	0.056	0.075
	Al tab	1.750	0.674	2.120	0.086	0.109

2.2 Apparatus

The friction coefficient tests were conducted on a Plint TE/77 High-Frequency tribometer, as shown in Figure 4 (a) at the High Temperature Materials Laboratory of Oak Ridge National Laboratory.

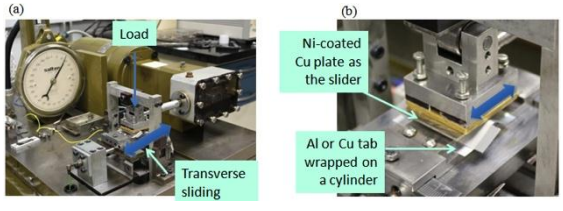

Figure 4 (a) Oscillating friction test machine; (b) a close-up view

The friction test configuration is shown in Figure 4 (b). On the top, the Cu coupon was fixed by four screws on a plate mounted on the end of a shaft that was driven by a Scotch yoke; and on the bottom, an Al or Cu tab was bent over a 6.4 mm diameter cylindrical steel pin under tension as shown in Figure 4 (b). The motivation of setting up the experiment by this way is two-fold. One is that the line-contact area is more uniform. The other is that the force transducer at one end of the lower specimen stage can accurately monitor the friction force in situ. In the experiment, the servo axis arm, along with the Cu coupon, moves reciprocally under a normal load (shown in Figure 4 (a)). The friction coefficient (μ) is continuously monitored and calculated using formula: $\mu = F_f / F_l$, where F_f is the friction force, and F_l is the normal load set by the user.

2.3 Experimental parameters

Different factors and levels for the experiments include surface conditions, sliding frequency, and normal load, as given in Table 2.

Table 2 Experimental parameters

Test type	Factors	Levels		
Cu tab with Cu coupon ("Cu test")	Normal load	20 N	20 N	60 N
	Sliding frequency	2 Hz	2 Hz	10 Hz
	Surface condition	As-received	Polished	Cleaned
Al tab and Cu coupon ("Al test")	Normal load	20 N	60 N	100 N
	Sliding frequency	2 Hz	2 Hz	10 Hz
	Surface condition	As-received	Polished	Cleaned

The 100N normal load was not chosen for the Cu tests because of the high friction forces that may damage the friction test machine through excessive force and vibrations. In addition, after the friction force exceeds the shear stress of a member of the friction pair and there is significant adhesive contact, the force of friction is a reflection of the shear stress of the bulk material and not the properties of the contact interface. Since the shear stress is only weakly affected by contact pressure (unless a high hydrostatic stress state exists), the friction force would remain relatively constant, causing a net reduction in friction coefficient as the applied load increases.

The as-received Cu coupon may have oil residues or contaminations on its surface. The coupons were cleaned using Acetone and Isopropanol to remove surface contaminations and oils. The polished coupons were polished using sand papers to remove the Nickel coating, whose surface roughness metrics (after polish) are listed in Table 3 (data shown were the averages from five polished coupons). For friction measurement, three repeats were performed, except for the polished surface condition where only one or two repeats were tested due to time constraints. For different experimental parameters, the test times varied from 20 to 90 seconds to ensure the tabs were not worn through. The data sampling rate for the tests was set to 200 points per second.

Table 3 Roughness measurement of the polished Cu coupon (unit: microns)

	Materials	R_p	R_v	R_z	R_a	R_q
Average	Polished Cu coupon	10.6	4.9	15.5	0.8	1.0
Standard deviation	Polished Cu coupon	1.6	0.9	1.3	0.1	0.1

3 EXPERIMENTAL RESULTS AND DISCUSSIONS

3.1 The friction coefficient results

Figure 5 shows a typical experimental result where the friction coefficient measurement is divided to three stages (S1, S2, and S3), defined as follows:

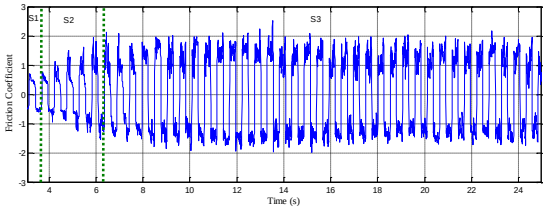

Figure 5 A typical example of experimental result

1) S1: The initial stage where the Cu coupon is sliding on the tab with no noticeable wear.
2) S2: An intermediate stage where the Cu coupon is sliding on the tab with noticeable wear on partial contact surface.
3) S3: A stage where the Cu coupon is sliding on the tab with noticeable wear on the whole contact surface, this stage is also called the steady-state stage since the friction coefficient becomes stabilized.

In Figure 5, friction coefficient data has to be rectified to reflect the reversal of the direction of the friction force as the upper specimen oscillates. The results of friction coefficient measurement may have included inertial effects and noises, particularly for about 15% of data at the beginning and 15% of data at the end of each half cycle. Therefore, our papered friction coefficients were

based on 70% of the data that fell during the mid-stroke.

Table 4 shows the experimental test results for the Cu tests. In the table, symbol * indicates that the final steady-state stage was never achieved due to the lack of stable wear conditions, while symbol ** indicates very short periods of S1 such that friction coefficients were not meaningful. Under either the as-received or polished conditions, the average friction coefficient between Cu coupons and Cu tabs ranges from 0.23 with a standard deviation of 0.02 (Stage S1) to 1.24 with a standard deviation of 0.07 (the steady-state stage). The friction coefficient reaches the final steady-state stage slowly. While, under the cleaned condition, the average friction coefficient between Cu coupons and Cu tabs is 1.18 with a standard deviation of 0.09 at the final steady-state stage. The friction coefficient reaches the final steady-state stage very quickly.

Table 4 Experimental test results for the Cu test

Surface conditions	Test ID	Sliding frequency (Hz)	Normal load (N)	Stage S1 duration (sec)	Stage S3 duration (sec)	Stage S1 friction Coefficient	Stage S3 friction Coefficient	Test Time (sec)
As-received	As-received 1	2	25	90	0	0.21	*	90
	As-received 2	2	25	90	0	0.22	*	90
	As-received 3	2	25	90	0	0.21	*	90
	As-received 4	2	60	24	0	0.22	*	90
	As-received 5	2	60	22	0	0.22	*	90
	As-received 6	2	60	90	0	0.21	*	90
	As-received 7	10	25	35	0	0.25	*	40
	As-received 8	10	25	35	0	0.24	*	40
	As-received 9	10	25	26	0	0.22	*	40
	As-received 10	10	60	< 2	36	**	1.22	40
	As-received 11	10	60	< 2	32	**	1.08	40
	As-received 12	10	60	12	0	0.23	*	40
Polished	Polished 1	2	25	24	0	0.23	*	90
	Polished 2	2	25	42	44	0.18	1.32	90
	Polished 3	2	60	65	14	0.28	1.25	90
	Polished 4	2	60	8	76	0.26	1.26	90
	Polished 5	10	25	7	31	0.24	1.45	40
	Polished 6	10	60	2	16	0.25	1.28	20
Cleaned	Cleaned 1	2	25	< 2	83	**	1.11	90
	Cleaned 2	2	25	< 2	84	**	1.22	90
	Cleaned 3	2	25	< 2	82	**	1.18	90
	Cleaned 4	2	60	< 2	86	**	1.07	90
	Cleaned 5	2	60	< 2	87	**	1.12	90
	Cleaned 6	2	60	< 2	85	**	1.18	90
	Cleaned 7	10	25	< 2	17	**	1.30	20
	Cleaned 8	10	25	< 2	18	**	1.26	20
	Cleaned 9	10	25	< 2	17	**	1.34	20
	Cleaned 10	10	60	< 2	18	**	1.15	20
	Cleaned 11	10	60	< 2	19	**	1.15	20
	Cleaned 12	10	60	< 2	19	**	1.06	20

Table 5 shows the experimental results for the Al tests. The average friction coefficient between Cu coupons and Al tabs (at the final steady-state stage) is 0.60 with a standard deviation of 0.06. The friction coefficient reaches the final steady-state stage very quickly. Surface conditions (as-received, polished, or cleaned) have no significant impact on the friction coefficients probably because the high applied load and resulting surface damage destroys the initial surfaces almost immediately.

Table 5 Experimental test results for the Al test

Surface conditions	Test ID	Sliding frequency (Hz)	Normal load (N)	Stage S1 duration (sec)	Stage S3 duration (sec)	Stage S1 friction Coefficient	Stage S3 friction Coefficient	Test Time (sec)
As-received	As-received 1	2	25	< 2	83	**	0.51	90
	As-received 2	2	25	< 2	81	**	0.55	90
	As-received 3	2	25	< 2	82	**	0.60	90
	As-received 4	2	100	< 2	68	**	0.49	90
	As-received 5	2	100	< 2	70	**	0.47	90
	As-received 6	2	100	< 2	69	**	0.50	90
	As-received 7	10	25	< 2	38	**	0.65	40
	As-received 8	10	25	< 2	38	**	0.67	40
	As-received 9	10	25	< 2	38	**	0.61	40
	As-received 10	10	60	< 2	36	**	0.59	40
	As-received 11	10	60	< 2	36	**	0.61	40
	As-received 12	10	60	< 2	36	**	0.58	40
Polished	Polished 1	2	25	< 2	86	**	0.68	90
	Polished 2	2	100	< 2	84	**	0.64	90
	Polished 3	10	25	< 2	32	**	0.65	40
	Polished 4	10	60	< 2	31	**	0.62	40
Cleaned	Cleaned 1	2	25	< 2	86	**	0.62	90
	Cleaned 2	2	25	< 2	85	**	0.56	90
	Cleaned 3	2	25	< 2	86	**	0.54	90
	Cleaned 4	2	100	< 2	88	**	0.59	90
	Cleaned 5	2	100	< 2	89	**	0.59	90
	Cleaned 6	2	100	< 2	88	**	0.56	90
	Cleaned 7	10	25	< 2	38	**	0.66	40
	Cleaned 8	10	25	< 2	37	**	0.66	40
	Cleaned 9	10	25	< 2	38	**	0.64	40
	Cleaned 10	10	60	< 2	37	**	0.63	40
	Cleaned 11	10	60	< 2	38	**	0.61	40
	Cleaned 12	10	60	< 2	38	**	0.61	40

3.2 Effect of surface conditions

The Cu tests

Figure 6 shows the typical evolution of the friction coefficient versus test time under different surface conditions (as-received, polished, and cleaned) for one test only at 25 N normal force. As shown in the figure, the surface conditions have substantial impact on the evolution of the friction coefficient.

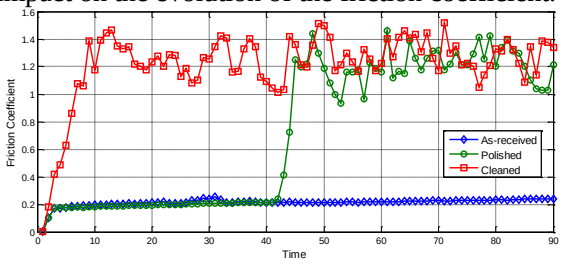

Figure 6 Friction coefficients versus time for the Cu test

Under the as-received condition, the friction coefficient increases gradually, but always stays on Stage S1 during the entire period of the experiment. This is due to relatively good lubrication from oil residues on the Cu surface, leading to very low friction coefficients. The figure also shows a small but gradual increase of friction coefficient at Stage S1, due to diminishing lubrication with time. Hence, at Stage S3, it is expected that the friction coefficient will eventually achieve steady-state after lubrication effects completely disappear. Under the polished condition, the friction coefficient also stays on Stage S1 for a considerable amount of time, and then rapidly goes to Stages S2 and S3. Compared with the as-received condition, it takes a relatively less amount of time for the polished coupons to be worn out. Under the cleaned condition, the friction coefficient increases rapidly at the beginning, and then stays on the steady-state stage (S3) with a constant friction coefficient.

Please note that Figure 6 shows one representative test sample only (normal load: 25 N, sliding frequency: 2 Hz) and does not represent the average results. Our test data shows that the friction data, both for the as-received and for the polished conditions, varies very significantly, especially under the different normal loads and sliding frequencies. In general, higher normal loads and sliding frequencies accelerate the progression from Stage S1 to Stages S2 and S3, as will be discussed later.

With respect to the effects on wear, Figure 7 illustrates the photos of representative tested Cu coupons and Cu tabs under three conditions, as-received, polished, and cleaned. As can be seen from the figure, the wear progression for the cleaned condition is most severe, and the wear under the as-received condition is the least. This result can be explained by the oil residues on the as-received Cu coupon. Relatively speaking, the effect of surface polishing is secondary.

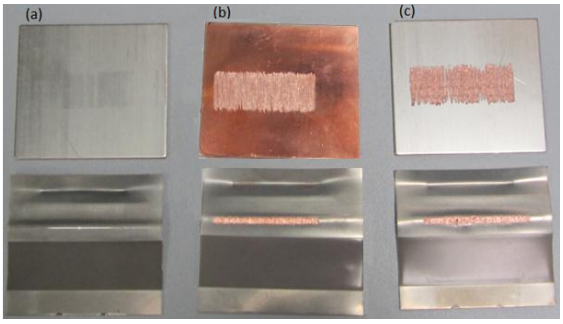

Figure 7 Photos of Cu coupons and Cu tabs after friction tests (a) as-received; (b) polished; (c) cleaned

The surface roughness of the Cu coupons and Cu tabs after friction tests was measured using a laser microscopic scanner, Keyence VK-9710. Figures 8 and 9 depict representative microscopic photos. Detailed roughness data is given in Table 6.

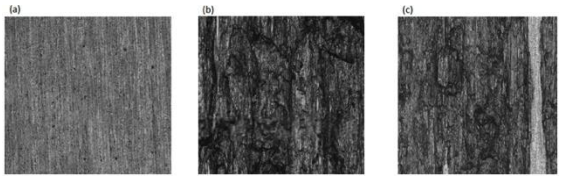

Figure 8 Microscopic photos of Cu coupons after friction tests (a) as-received; (b) polished; (c) cleaned

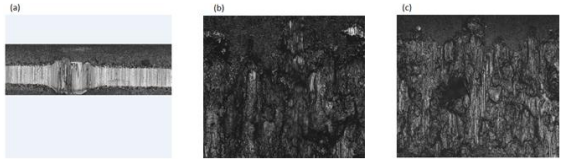

Figure 9 Microscopic photos of Cu tabs after friction tests (a) as-received; (b) polished; (c) cleaned

Table 6 Roughness measurements of tested Cu tabs and Cu coupons (unit: microns)

Materials	Surface Conditions	R_p	R_v	R_z	R_a	R_q
Cu tabs	As-received	17.3	10.5	27.7	1.9	2.4
	Polished	71.3	85.3	156.6	15.4	20.1
	Cleaned	119.6	121.0	240.7	26.0	33.0
Cu coupons	As-received	12.7	12.7	25.4	1.3	1.7
	Polished	72.5	60.1	132.6	10.6	13.8
	Cleaned	83.7	61.2	144.9	11.0	14.9

The Al tests

As shown in Figure 10, surface conditions do not have a substantial impact on the evolution of the friction coefficient as they have for the Cu test. Under all three conditions, the friction coefficient increases rapidly at the beginning of the experiment, and then stays on a relatively steady-state stage (S3). In addition, the friction coefficient under the polished condition is a little larger than the ones under the as-received and cleaned conditions. As previously discussed by one of the authors [14], the shapes of friction versus time or cycles plots can reveal information about the details in the interface. The polished and as-received surfaces show a gradual rise to steady-state suggesting, respectively, the gradual removal of films (as-received), or the gradual roughening of smooth surfaces (polished). The rise and drop of the cleaned specimen suggests a sequence of rapid abrasion of the initial aluminum oxide to expose a more adhesive material underneath which, under the friction force deformed to produce a textured microstructure whose easy shear direction was aligned to the sliding direction causing friction to come down again, and eventually reaching a steadier long-term friction behavior.

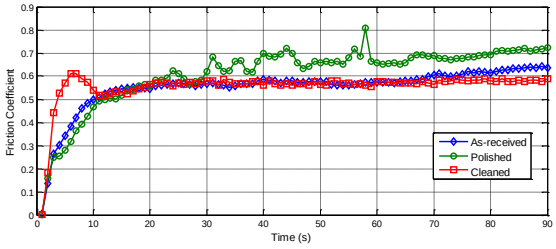

Figure 10 Friction coefficients versus the test time for the Al tests

Figure 11 shows photos of three representative tested specimens after the friction tests. As can be seen, the wear on the surfaces of both Cu coupons and Al tabs under the three tested conditions is comparable.

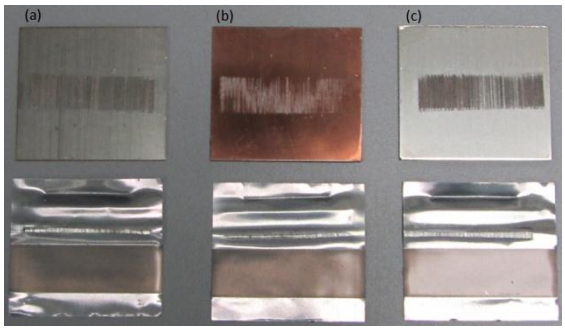

Figure 11 Microscopic photos of Cu coupons and Al tabs after the friction tests (a) as-received; (b) polished; (c) cleaned

Figures 12 and 13 depict representative microscopic photos of Cu coupons and Al tabs, respectively. Detailed surface roughness data is given in Table 7.

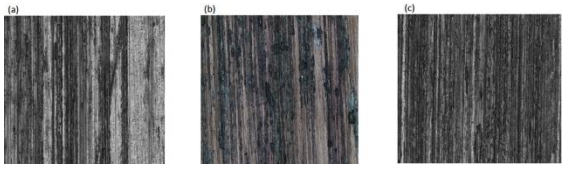

Figure 12 Microscopic photos of Cu coupons after the friction tests (a) as-received; (b) polished; (c) cleaned

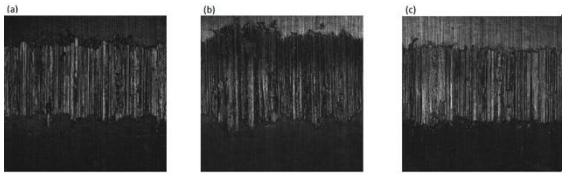

Figure 13 Microscopic photos of Al tabs after the friction tests (a) as-received; (b) polished; (c) cleaned

Table 7 Roughness measurement of tested Cu coupons and Al tabs

Materials	Surface Conditions	R_p	R_v	R_z	R_a	R_q
Al tabs	As-received	59.5	62.5	122.0	15.2	18.4
	Polished	67.8	76.3	144.1	19.3	24.6
	Cleaned	58.1	48.3	106.4	13.2	16.1
Cu coupons	As-received	32.9	16.4	49.3	2.1	2.9
	Polished	45.9	19.1	65.0	2.2	3.6
	Cleaned	40.2	36.0	76.2	3.5	5.1

3.3 Effect of normal load

Figures 14 and 15 show the averaged friction coefficient progression for all the tests under different conditions of normal loads. As indicated in Tables 4 and 5, all tests were preset with different test duration, to ensure that the tab was not worn through to damage the friction tester. Hence, in Figures 14 and 15, the steady-state results were extrapolated beyond the worn-through conditions until 90 seconds.

Figure 14 shows the average friction coefficient versus the test time under different normal loads and surface conditions for Cu tests. As can be seen from the figure, there are no obvious effects of normal loads except for the as-received condition where a lower normal load results in lower friction coefficient. The result can be explained by that, under the as-received condition, a high normal load expedites the evolution of the friction coefficient from Stage S1 to Stages S2 and S3. The figure also implies that higher normal load accelerates the wear process.

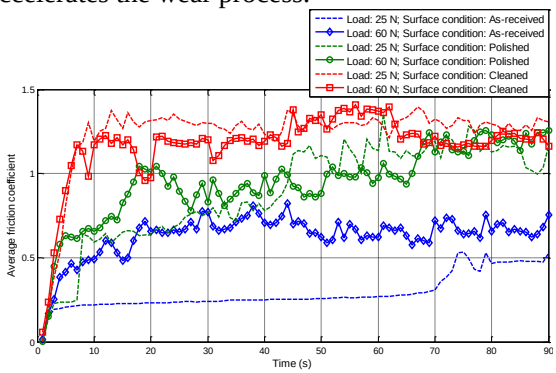

Figure 14 Average friction coefficients versus the test time for the Cu test

Figure 15 shows the average friction coefficient versus the test time for Al tests. As shown from the figure, the effects of normal loads on friction coefficient, after 30 seconds of sliding, are barely noticeable except under the polished condition, where higher normal loads result in higher friction coefficient at the early stage of experimental tests, but the effect gradually diminishes.

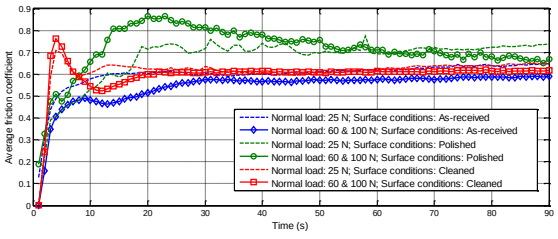

Figure 15 Average friction coefficients versus the test time for the Al test

3.4 Effect of sliding frequency

Figures 16 and 17 show the averaged friction coefficient for all the tests under two different sliding frequencies. In the figures, the steady-state results were extrapolated beyond the worn-through conditions until 90 seconds.

With respect to the Cu test, Figure 16 shows sliding frequency has a tangible impact on friction coefficient, especially for the polished and as-received conditions. The result can be explained by that higher sliding frequency accelerates the evolution of friction coefficient from Stage S1 to Stages S2 and S3. When it comes to the effects of sliding frequency on Stage S3 specifically, the sliding frequency has no significant impact on friction coefficient.

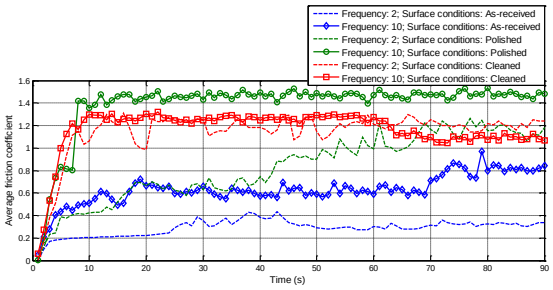

Figure 16 Average friction coefficients versus the test time for the Cu test

Figure 17 shows the friction coefficient versus the test time under different frequency and surface conditions for Al tests. As can be seen, there are no obvious effects from different frequency except for the polished condition.

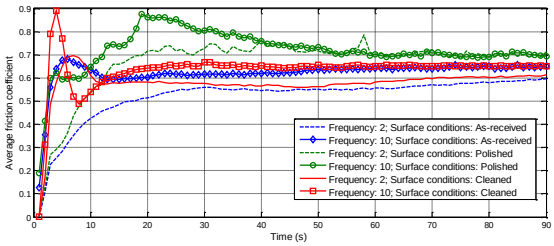

Figure 17 Average friction coefficients versus the test time for the Al test

4 Ultrasonic Welding Simulations

This section, we briefly describe a hybrid finite element analysis case study of ultrasonic welding for battery tabs. Friction coefficient is the key model parameter to predict realistic workpiece temperatures using the finite element procedure described in [13]. It is a three tabs + one interconnect welding configuration, as illustrated in Fig. 18. Some of the key data are summarized in Table 8, and the tab and interconnect coupon thicknesses are 0.2 mm and 1.0 mm, respectively.

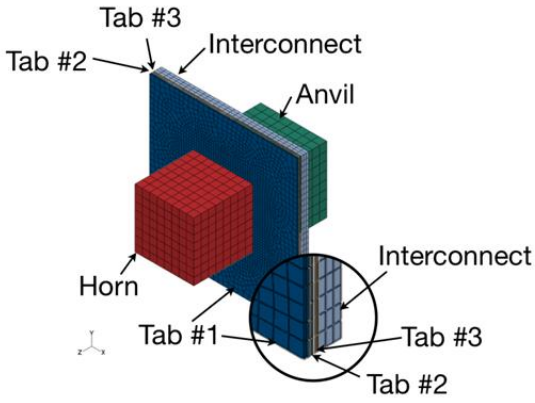

Figure 18 Geometry configuration with a horn, anvil, three 0.2 mm thick tab foils and one 1.0 mm thick interconnect coupon.

Table 8 Experimentally measured final temperatures, corresponding ultrasonic welding conditions, and friction coefficient and the fraction η of Eq. (9) for two ultrasonic welding configurations.

	3 Cu foils + 1 Interconnect	3 Al foils + 1 Interconnect
Clamping pressure	80 MPa	30 MPa
Welding amplitude, u_0	24 μm	12 μm
Welding time	500 ms	500 ms

Different thermal conditions of workpieces illustrated in Fig. 18 are considered in the simulations. The conditions include ultrasonic welding processes with insulated anvil, preheated interconnect coupon and a coupon thinner than 1.0 mm. The preheated coupon is implemented by assigning an initial temperature condition of 100 °C to the anvil. Finally, the thinner coupon is implemented by remodeling the coupon thickness as 0.4 mm.

Temperature contours and histories at the end of 500 ms ultrasonic welding process are shown in Figs. 19 and 20. It can be seen from the figures that the thin coupon case results in the highest final temperature. It can also be seen from Fig. 19(b) that the gap conductance reduction effectively implemented the insulated condition for the anvil.

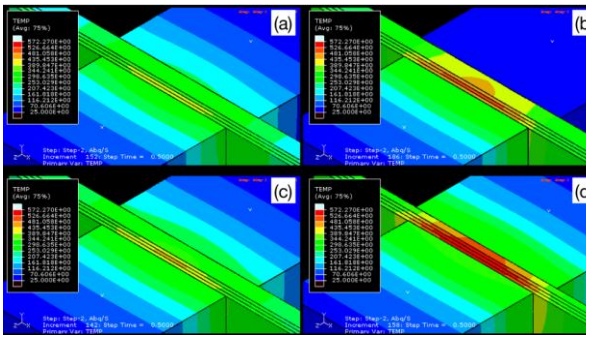

Figure 19 Temperature contours at the end of a 500 ms ultrasonic welding step for (a) default configuration, (b) insulated anvil, (c) preheated coupon and (d) thin coupon.

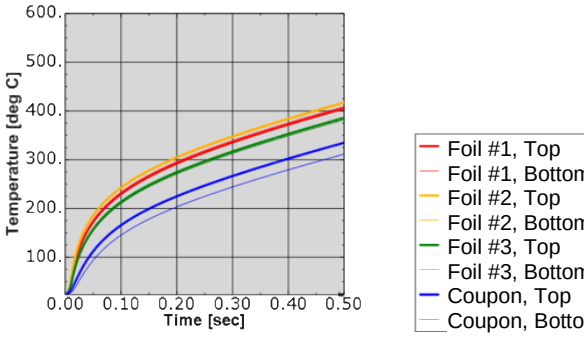

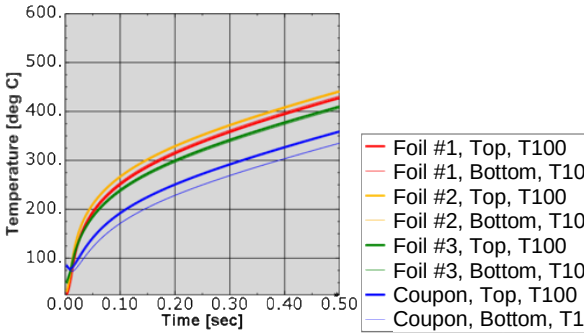

Figure 20 Temperature histories at the end of a 500 ms ultrasonic welding step for (a) default configuration, (b) insulated anvil, (c) preheated coupon and (d) thin coupon.

5 Summary and Conclusions

In this study, friction coefficients between battery tabs and Cu coupons, and the effects of surface conditions, sliding frequency, and normal load on the friction coefficient were studied using a reciprocating sliding apparatus. Experimental tests were performed under the following conditions:

1)Surface condition: As-received, polished, and cleaned
2)Sliding frequency: 2 Hz and 10 Hz
3)Norml load: 20 N and 60 N for the Cu test; 20 N, 60 N, and 100 N for the Al test.

According to the experimental tests, sliding behaviors between battery tabs and Cu coupons can be classified into three stages where the friction coefficient ranges from a relatively low value to a high value. Surface conditions have bigger impacts on the friction coefficient between Cu tabs and Cu coupons when compared with the one between Al tabs and Cu coupons. Specifically, under both the as-received and the polished conditions of the Cu test, the friction coefficient stays on the initial stage for a considerable amount of time, and reaches the final steady-state stage slowly. However, for all other test conditions (include the Al test), the friction coefficient reaches the final steady-state stage very quickly. In addition, normal load and sliding frequency have no significant impact on the steady-state friction coefficient, but higher normal load and sliding frequency substantially accelerate the wear process.

The following conclusions can be drawn:

1)The average friction coefficient between a Cu bus-bar (either as-received or polished) and a Cu tab is 1.24 (steady-state value). The friction coefficient reaches the final steady-state stage relatively slowly.
2)The average friction coefficient between a Cu bus-bar (under the cleaned surface condition) and a Cu tab is 1.18 (steady-state value). The friction coefficient reaches the final steady-state stage very quickly.
3)The average friction coefficient between a Cu bus-bar and an Al tab is 0.60 at the final steady-state stage. Surface conditions (as-received, cleaned, or polished) have little impact on the friction coefficient. The friction coefficient reaches the final steady-state stage very quickly.
4)Normal load and sliding frequency have no significant impact on the friction coefficient, but higher normal load and sliding frequency substantially accelerate the wear process.
5)Finite element analyses were successfully simulated to predict the temperature and quality of the ultrasonic welds for battery tabs.

Acknowledgments

This study was partially sponsored by U.S. Government under an Agreement/Project DE-EE0002217, Department of Energy Recovery and Reinvestment Act of 2009, Battery Pack Manufacturing. It was also sponsored in part by

the U.S. Department of Energy, Assistant Secretary for Energy Efficiency and Renewable Energy, Office of Vehicle Technologies, as part of the High Temperature Materials Laboratory User Program at the Oak Ridge National Laboratory.

Disclaimer

References

[1] Zhang, C., and Li, L., 2009, "A Coupled Thermal-Mechanical Analysis of Ultrasonic Bonding Mechanism," Metallurgical and Materials Transactions B, 40(2), pp. 196-207.

[2] Lee, S. S., Kim, T. H., Hu, S. J., Cai, W., Abell, J. A., and Li, J., 2012, "Characterization of Ultrasonic Metal Weld Quality for Lithium-Ion Battery Tab Joining," ASME Journal of Manufacturing Science & Engineering, 135(2), 22 March 2013, 021004.

[3] Kang, B., Cai, W., and Tan, C.A., 2013, "Dynamic Response Of Battery Tabs Under Ultrasonic Welding," accepted by ASME Journal of Manufacturing Science & Engineering.

[4] Lee, D, Kannatey-Asibu, Jr., E., and Cai, W., 2013, "Ultrasonic Welding Simulations for Multiple, Thin and Dissimilar Metals," accepted by ASME Journal of Manufacturing Science & Engineering.

[5] Siddiq, A., and Ghassemieh E., 2008, "Thermomechanical Analyses of Ultrasonic Welding Process Using Thermal and Acoustic Softening Effects," Mechanics of Materials, 40(12), pp. 982-1000.

[6] Jairo, A. M., Kövesdy, I., and Bressan, J. D., 2010, "Experimental Kinetic Friction Coefficient (μk) Determination in the Interface Polycarbonate Blade and Flat Rubber-belt when Interacting with Ore, Lubricant and Pressure," International Journal of Mining and Mineral Engineering, 2(2), pp. 159-167.

[7] Qu, J., Truhan, J. J., Blau P. J., and Ott, R., 2007, "The Development of a "Pin-on-Twin" Scuffing Test to Evaluate Materials for Heavy-Duty Diesel Fuel Injectors," Tribology Transactions, 50(1), pp. 50-57.

[8] Guermazi, N., Elluech, K., Ayedi, H. F., Fridrici V., and Kapsa P., 2009, "Tribological Behaviour of Pipe Coating in Dry Sliding Contact with Steel," Materials and Design, 30(8), pp. 3094-3104.

[9] Lee, J. H., Xu, G. W., and Liang, H., 2001, "Experimental and Numerical Analysis of Friction and Wear Behavior of Polycarbonate," Wear, 251(2), pp. 1541-1556.

[10] Siddiq, A. and Ghassemieh, E., 2008, "Thermomechanical analyses of ultrasonic welding process using thermal and acoustic softening effects," Mechanics of Materials, 40, pp. 982 - 1000.

[11] Elangovan, S., Semeer, S. and Prakasan, K., 2009, " Temperature and stress distribution in ultrasonic metal welding – An FEA-based study," Journal of Material Processing Technology, 209, pp. 1143 - 1150.

[12] Zhang, C. and Li, L., 2009, "A coupled thermal-mechanical analysis of ultrasonic bonding mechanism," Metallurgical and Materials Transactions B, 40B, pp. 196 - 207.

[13] Lee, D, Kannatey-Asibu, Jr., E., and Cai, W., 2013, "Ultrasonic Welding Simulations for Multiple, Thin and Dissimilar Metals," accepted by ASME Journal of Manufacturing Science and Engineering.

[14] Blau, P. J. (1981) "Interpretations of the Break-in Behavior of Metals in Sliding Contact," Wear, Vol. 71, p. 29.

Authors

Dr. Wayne Cai is a Staff Researcher at General Motors Global R&D Center in Warren, Michigan, USA. He is recognized for his innovativeness in lithium-ion battery manufacturing, with twenty-one US and international patents (or patents pending) and many GM trade-secrets inventions. He authored over fifty peer-reviewed research papers. He received Ph.D. from The University of Michigan.

Dr. Peter J. Blau is a Fellow of ASM, ASTM, and STLE. He author or co-authored four books and over 160 journal articles. Specializing in the materials aspects of friction and wear, he is currently a Distinguished R&D Staff Member in the Materials Science and Technology Division, Oak Ridge National Laboratory (ORNL) in Oak Ridge, Tennessee. He earned a Ph.D. from The Ohio State University.

Dr. Jun Qu is a Senior R&D staff scientist at Oak Ridge National Laboratory. He earned his Ph.D. from North Carolina State University in 2002. He has published 3 book chapters, 58 peer-reviewed journal papers, and 8 granted or pending U.S. patents. Dr. Qu received the Outstanding Young Manufacturing Engineer Award from the SME in 2009 and currently serves as a Technical Editor for Tribology & Lubrication Technology.